PROTEINS
STRUCTURE ■ FUNCTION ■ BIOINFORMATICS

The peculiar structural features of kiwi fruit pectin methylesterase: Amino acid sequence, oligosaccharides structure, and modeling of the interaction with its natural proteinaceous inhibitor

M. Antonietta Ciardiello,[1]* Rossana D'Avino,[1] Angela Amoresano,[2] Lisa Tuppo,[1] Andrea Carpentieri,[2] Vito Carratore,[1] Maurizio Tamburrini,[1] Alfonso Giovane,[3] Piero Pucci,[2] and Laura Camardella[1]

[1] Institute of Protein Biochemistry, C.N.R., 80131 Napoli, Italy

[2] Department of Organic Chemistry and Biochemistry, University Federico II of Napoli, 80126 Napoli, Italy

[3] Department of Biochemistry and Biophysics, Second University of Napoli, 80138 Napoli, Italy

ABSTRACT

Pectin methylesterase (PME) from kiwi fruit (Actinidia deliciosa) is a glycoprotein, showing an apparent molecular mass of 50 kDa upon size exclusion chromatography and SDS-PAGE. The primary structure, elucidated by direct sequencing of the protein, comprises 321 amino acid residues providing a molecular mass of 35 kDa. The protein has an acetylated Thr residue at the amino terminus and five N-glycosylation consensus sequences, four of which are actually glycosylated. A careful investigation of the oligosaccharide structures demonstrated that PME glycans belong to complex type oligosaccharides essentially consisting of xylosylated polyfucosylated biantennary structures. Alignment with known mature plant PME sequences indicates that the postulated active site residues are conserved. Kiwi PME activity is inhibited following the interaction with the proteinaceous inhibitor PMEI, isolated from the same source. Gel-filtration experiments show that kiwi PME/PMEI complex is stable in a large pH range and dissociates only at pH 10.0. Modeling of the interaction with the inhibitor was performed by using the crystal structure of the complex between kiwi PMEI and tomato PME as a template. The model shows that the binding site is the same reported for tomato PME. However, additional salt link interactions are found to connect the external loops of kiwi PME to PMEI. This finding may explain the higher pH stability of the complex formed by the two kiwi proteins respect to that formed by PMEI and tomato PME.

INTRODUCTION

Pectin methylesterase (PME) (EC 3.1.1.11) catalyzes the hydrolysis of the methyl group in the C6 position of galacturonic acid units of pectin, yielding acidic pectin and methanol. Pectin is a main component of the primary cell wall and of the middle lamella in higher plants, and is involved in important physiological processes such as cell extension and development, fruit ripening, interaction with the environment, and so forth.[1] Pectin is secreted as a highly methylesterified form into the cell wall, where it is deesterified by PMEs. The action of PME can provide two opposite effects, that is, either stiffening of the cell wall by producing blocks of unesterified carboxyl groups that can interact with calcium ions forming a pectate gel, or cell wall loosening due to the proton release that can stimulate the activity of cell wall hydrolases.

Several PME isoforms with different biochemical properties are either constitutively or differentially expressed in specific plant tissues and at specific developmental stages.[1–4] Recently, sequencing of *Arabidopsis* genome allowed the identification of 67 PME-related genes in this species.[5] Most of plant PMEs are encoded as precursors, bearing at the N-terminus the signal peptide and a large proregion (consisting of about 250 amino acid residues), which is cleaved off to yield the mature enzyme. The function of the proregion is as yet unknown. Several possible roles, such as PME intramolecular chaperone,[1] correct targeting of PME toward the cell wall,

and inhibition of its activity before processing to mature protein,[1,6] have been suggested.

The discovery in kiwi fruit of a proteinaceous inhibitor (PMEI) of PME suggested a possible mechanism of regulation of the mature enzyme activity.[7] Kiwi PMEI is a monomeric protein of 152 amino acid residues, with a pI of 4.5. Its amino acid sequence shows significant similarity with plant β-fructofuranosidase inhibitors[8] and with the N-terminal proregion of plant PMEs.[9] Recently, the structural determinants of the interaction between PME and its inhibitor have been investigated by crystallization and analysis of the complex formed by kiwi fruit PMEI and tomato fruit PME, chosen as a representative plant PME.[10] The enzyme folds into a right-handed parallel β-helix, as already shown for PME from the bacterium *Erwinia chrysanthemi*[11] and from carrot root.[12] This structure, described for the first time in pectate lyase,[13] is common to several pectin modifying enzymes. The crystallographic structure shows that the arginine and the two aspartic acid residues, postulated to be involved in the catalytic activity, are located on the surface of the β-helix in a cleft formed by protruding loops, suitable for pectin binding. Kiwi PMEI folds as a four α-helix bundle bearing an unusual N-terminal hairpin-like helical extension, similar to the inhibitor of β-fructofuranosidase from tobacco[14] and PMEI from *Arabidopsis*.[15] The structure of the PME/PMEI complex shows that the inhibitor binds PME covering the shallow cleft where the putative active site of the enzyme is located. The interaction interface is large and displays a high polar character, typical of nonobligate complexes of soluble proteins, which need to expose a hydrophilic surface in their uncomplexed form.[10]

Kiwi fruit PME was initially overlooked because of the presence of PMEI in the tissue. It was then purified from the cell wall fraction of incompletely ripened fruit, where PMEI was present in lower amount.[2,16,17] Kiwi fruit PME is active in the entire pH range studied (5.0–8.5), with two maxima at 6.5 and 8.0–8.5. In the acidic pH range, a strong salt dependent activity was observed.[17] Kiwi PME activity is inhibited by PMEI. Surface plasmon resonance (SPR) experiments indicate the binding to occur up to pH 9.5, and the inhibitor to be completely released only by raising the pH to 10.0.[17]

The enzyme is a monomer, with an apparent molecular mass (∼50 kDa) higher than that of most plant PMEs (32–35 kDa). A molecular size higher than 35 kDa has been reported for PMEs such as TT-PME from orange,[18] PMEα from mung bean hypocotyl,[19] and the acidic PME from jelly fig achene,[20] for which glycosylation was suggested. Kiwi PME is reported to be a glycoprotein since it is positively stained by the Schiff reagent after SDS-PAGE and binds to a concanavalin A-Sepharose column.[2]

In the framework of the study of the interaction between PMEI and PME from the same source, we report here the structural characterization of PME from kiwi fruit. The characterization comprises: (i) primary structure elucidation by direct protein sequencing, (ii) oligosaccharide characterization by mass spectrometry analysis, and (iii) modeling of the enzyme structure in complex with PMEI.

METHODS

Kiwi fruits were collected at the Botanical Garden of the University of Naples Federico II, peeled, and stored at −80°C. Trypsin was from Sigma (Milan, Italy) or Boehringer (Mannheim, Germany), chymotrypsin and pepsin were from Boehringer; bovine serum albumin, dithiothreitol, Tris, 4-vinylpyridine, iodoacetamide, glycerol, and thioglycerol from Sigma; DEAE-cellulose (type DE52) and SP-Sepharose from Whatman (Brentford, UK). Peptide N-glycosidase A (PNGase A) was from Roche (Monza, Italy). Prepacked PD-10 gel-filtration cartridges were from Pharmacia (Milan, Italy). Prepacked Sep-pak C_{18} cartridges were purchased from Waters (Milan, Italy). Sequencer-grade reagents were from Applied Biosystems (Foster City, CA). All other reagents were of the highest commercially available quality.

Enzyme activity

PME activity was routinely measured following the decrease of pH upon demethylesterification of pectin using bromothymol blue as indicator. The assay solution contained 0.1% citrus pectin in $0.1M$ NaCl, adjusted to pH 7.5–8.0 with NaOH. Specific activity was determined on a MeterLab PHM 290 pH-stat equipped with a ABU 901 autoburette and a SAM 90 sample station (Radiometer, Copenhagen), at room temperature (∼20°C), in 5 mL sample solution containing 0.2 μg of enzyme, 0.1% citrus pectin, $0.1M$ NaCl and 10 mM Tris-HCl buffer pH 7.5. Titration of released protons was carried out with 10 mM NaOH. One activity unit is defined as the amount of enzyme releasing 1 μmole of protons per minute.

SDS-PAGE

SDS-PAGE was carried out in the Bio-Rad (Segrate, Italy) Mini Protean apparatus, using 15% polyacrylamide gels. Staining was carried out in 0.02% Coomassie R-250 Brilliant Blue in 10% acetic acid/25% isopropanol; rinsing was performed in 10% acetic acid/25% methanol.

Protein purification

Kiwi fruits were homogenized in water. The pH of the homogenate was 3.5. After centrifugation, the supernatant was discarded and the pellet, containing the cell wall fraction, was collected and homogenized again in the presence of $0.5M$ NaCl, adjusted to pH 8.3. The PME activity was recovered in the salt extract of the cell wall,

similar to most PMEs so far described.[1] The extract, dialyzed against 10 mM Tris-HCl, pH 7.5, was loaded on a DE52 column equilibrated in the same buffer. The protein was eluted in the column flow-through, which was adjusted to pH 5.0 and loaded on a SP-Sepharose column, equilibrated in 10 mM sodium acetate, pH 5.0 (buffer A). Elution was carried out by increasing the concentration of buffer B (50 mM sodium acetate, pH 5.0, containing 0.5M NaCl). The fractions containing the PME activity were pooled, dialyzed against 10 mM sodium acetate, pH 5.0, and further purified by FPLC ion-exchange chromatography carried out on a Mono-S HR 10/10 column (Amersham-Pharmacia, Milan, Italy), equilibrated in the same buffer (buffer A). Flow-rate was 3 mL/min. Elution was carried out increasing the concentration of buffer B, as above. The absorbance was recorded at 280 nm. The pure protein was finally obtained by elution from a gel-filtration column Superdex 75 HR 10/30 (Amersham-Pharmacia) equilibrated in 50 mM Tris-HCl, pH 7.5, containing 0.25M NaCl.

When needed, protein samples were concentrated by ultrafiltration using Centriplus YM-30 filters (Millipore, Bedford, MA).

Protein concentration was determined by the Bio-Rad Protein Assay, using calibration curves made with bovine serum albumin.

Denaturation and alkylation

The protein was dissolved at a concentration of 10 mg/mL in 0.5M Tris-HCl pH 8.0, containing 2 mM EDTA and 6M guanidine hydrochloride. Dithiothreitol (10-fold molar excess over the thiol groups of the protein) was added, and the solution was kept at 37°C for 2 h. Iodo-acetamide or 4-vinylpyridine (fivefold molar excess over the total thiols) was then added and the mixture was kept in the dark at room temperature for 30 min. At the end of the reaction, reagents were removed by gel filtration on a PD-10 column equilibrated with 0.1% trifluoroacetic acid.

Amino acid sequencing

Trypsin and chymotrypsin digestions of PME were carried out at an enzyme:PME ratio of 1:20 (w/w) in 0.1M Tris-HCl, pH 8.5 and 0.1M Tris-HCl, pH 7.8, containing 10 mM CaCl$_2$, respectively, at 37°C for 14 h. Pepsin digestion of the tryptic fragment T20 was carried out at an enzyme:protein ratio of 1:70 (w/w) in 5% formic acid, at 37°C for 2 h.

Cleavage of Asp-Pro bonds was performed on polybrene-coated glass-fiber filters in 70% (v/v) formic acid, for 24 h at 42°C.[21] The Asp-Pro-cleaved peptide was treated with *o*-phthalaldehyde (OPA) before sequencing[22] in order to block the non-Pro N-terminus and reduce the background.

Separation of peptides was accomplished by reverse-phase HPLC on a μBondapak-C$_{18}$ column (Waters, 3.9 × 300 mm), using 0.1% trifluoroacetic acid and 0.08% trifluoroacetic acid in acetonitrile as eluents. The eluate was monitored at 220 and 280 nm. The separated fractions were manually collected and sequenced. Unblocking of the N-terminal residue was achieved by incubation in 30% trifluoroacetic acid at 55°C for 2 h.

Amino acid sequencing was performed with an Applied Biosystems Procise 492 automatic sequencer, equipped with on-line detection of phenylthiohydantoin amino acids. Protein sequence analyses were performed using softwares available on the ExPASy Proteomics Server (www.expasy.org).

Analysis of the complex formation by size exclusion chromatography

PME aliquots corresponding to 0.2 nmoles were mixed with 1.2 nmoles of PMEI[16] and incubated for 15 min at room temperature in the following incubation buffers: 10 mM bis-Tris-HCl, pH 6.0; 10 mM Tris-HCl, pH 7.5 and 8.5; 10 mM CAPS-NaOH, pH 10.0. The samples were then loaded on a gel-filtration column Superdex 75 HR 10/30, equilibrated and eluted with the incubation buffer containing 0.25M NaCl. Fractions of 0.5 mL were collected at a flow rate of 0.5 mL/min. The absorbance at 280 nm was recorded. Aliquots of the fractions containing the complex, corresponding to 0.2 and 2 μg of PME, were used for the PME activity assay and for SDS-PAGE analysis, respectively.

Oligosaccharide characterization

Reduced and carboxyamidomethylated PME was digested with trypsin (Sigma) in 50 mM ammonium bicarbonate, pH 8.5, using an enzyme/substrate ratio of 1:25 (w:w) for 6 h at 37°C. Deglycosylation of the peptide mixtures was performed by treatment with PNGase A in 50 mM ammonium bicarbonate, pH 8.5, overnight at 37°C using 0.1 enzyme unit per 300 μg of protein. N-linked oligosaccharide chains released by PNGase A were separated from peptides by reverse phase chromatography on prepacked Sep-pak cartridges.

Mass spectrometry

Positive Reflectron MALDI spectra and MALDI-PSD spectra were recorded on a Voyager DE STR Pro instrument (Applied Biosystems, Framingham, MA). The MALDI matrices were prepared by dissolving 20 mg of DHB or 10 mg of α-cyano (α-cyano-4-hydroxycinnamic acid) in 1 mL of acetonitrile/0.1% trifluoroacetic acid (70:30 v/v). Typically, 1 μL of matrix was applied to the metallic sample plate and 1 μL of analyte was then added. Acceleration and reflector voltages were set up as follow: target voltage at 20 kV, first grid at 95% of target

voltage, delayed extraction at 600 ns. The PSD fragment spectra were acquired after pseudomolecular cation selection using the time ion selector. Fragment ions were refocused by stepwise reducing the reflector voltage by 20%. The individual segments were then stitched together using the Applied Biosystems software.

Sequence alignment and model building

Multiple sequence alignment of kiwi PME with other plant PMEs was performed with ClustalW. Comparative modeling was performed on a Silicon Graphics O2 workstation by using Homology[23] and MODELER[24] softwares in the Insight II molecular modeling system (Accelrys, San Diego, CA). The model of kiwi PME was built by using the carrot homologous enzyme (PDB code 1GQ8) as a structural template. Sequence alignment of the two proteins, sharing 58% identity, was submitted to MODELER for minimization. Loop regions were further refined with an optimization protocol comprising molecular dynamics simulated annealing. A set of 15 kiwi PME models was generated. Another set was obtained using the same program containing the information needed by MODELER to generate disulfide bonds.

A seven-sugar oligosaccharide (NAG-FUC-NAG-MAN-XYS-MAN-MAN) was bound, by using the Biopolymer program (Accelrys), to each one of the four Asn residues found to be glycosylated in kiwi PME. Oligosaccharide coordinates were taken from the 1.95 Å resolution crystal structure of *Erythrina corallodendron* lectin (PDB code 1AX1). The oligosaccharide structure was thus used as it is, avoiding further minimizations, since it was reported that after careful molecular dynamic simulation, performed to model the flexibility of the lectin sugar chain, the oligosaccharide had an average conformation very similar to that observed in the crystal structure.[25] Manual rotamer search for the Asn residues carrying the oligosaccharide was performed in order to find the best spatial position of each glycan chain.

Kiwi PME/kiwi PMEI complex was built by using the crystal structure of tomato PME/kiwi PMEI complex (PDB code 1XG2) as a template. Kiwi PME has only five more residues at the N-terminus and one less at the C-terminus compared to the tomato enzyme. The remaining 315 amino acid residues can be aligned without any internal gap. The two sequences are 56.5% identical. The kiwi PMEI sequence used for complex building contained all the 152 residues of the native protein. The alignment submitted to MODELER for minimization and simulated annealing generated 15 models of the complex. The protocol comprised careful refinement for loop regions.

Analysis of the structural violations of the probability density function (PDF) was performed for each model structure. The phi and psi torsion angles of the residues were evaluated by Ramachandran plot using the Swiss-PdbViewer program.

RESULTS

Purification

PME was purified from kiwi (*Actinidia deliciosa*) fruit samples, collected at the initial ripening stage, following the procedure described in the Materials and Methods section. The recovery of the electrophoretically pure PME with a specific activity of ∼2000 units/mg at pH 7.5 was 1 mg/1 kg of fruit.

Primary structure

Attempts to obtain the N-terminal sequence by automated Edman degradation of the native protein were unsuccessful, suggesting a blocked N-terminus. The primary structure was elucidated by automated sequencing of peptides deriving from chemical and enzymatic digestion of S-pyridylethylated protein.[26] Most of the PME primary structure was obtained by aligning peptides from trypsin digestion (see Fig. 1). Only the peptides necessary to elucidate the complete amino acid sequence are indicated. They were aligned by homology with other plant PMEs.

Sequencing of the N-terminal peptide (T1) did not produce any identifiable residue confirming the presence of a blocked N-terminus. Unblocking treatment, carried out as described in the Materials and Methods section,

```
   1                      25                            50
Ac-TAVTDIVPDVVVAKDGSGNFTTVGAAVAAAKDSSTARFVIYIKEGAYFEY
   <-----T1-----><-------T2------><-T3-><-T4--><-----

                          75                           100
   VDVDKKKTNLMFIGDGIGKTWIKGNRSVVDGWTTFRSSTVAVVGTGFIAR
   -T5---><----T6----><--T7-><----------T8---------->
                             <----K1--->

                         125                           150
   GISFENYAGPSKHQAVALRSGADFSAFYQCSFVGYQDTLYVHSLRQFYSE
   <----T9----><-T10-><-----------T11----------><----

                         175                           200
   CDVYGTIDFIFGNAAAVLQKCNLYARKPNENQKNIFTAQGRDDPNQNTGI
   -------T12---------><-T13><-T14-><--T15-><--------

                         225                           250
   SILNCKVAAAADLIPVLSSFKTYLGRPWKEYSRTVFLLSQMESLIDPAGW
   -T16-><-----T17-----><--T18-> T19<--------T20-----
                                                   <--

                         275                           300
   LEWSGDFALTTLYYREYKNTGPGSNTTARVTWPGYAVTTNETEVIQFTVG
   ----**********>T21<---T22---><--------------------
   --DP--------><-TP->

   NFIQGSQWLTSYNIPVYLNLT
   --T23--------><--T24--->
```
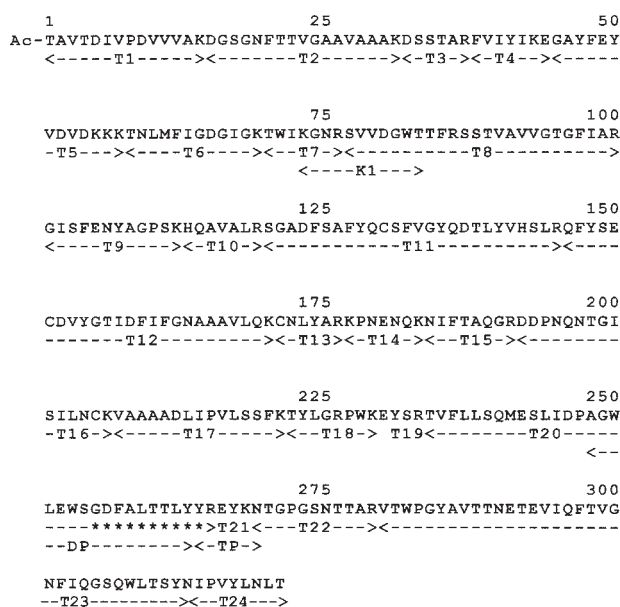
Figure 1

Amino acid sequence of kiwi fruit PME. Arrows indicate fragments obtained by enzymatic digestion with trypsin (T), trypsin followed by pepsin (TP), chymotrypsin (K), and by acidic chemical treatment (DP). Asterisks indicate the region of peptide T20 not entirely sequenced. Peptides from each digestion are numbered according to their order in the sequence.
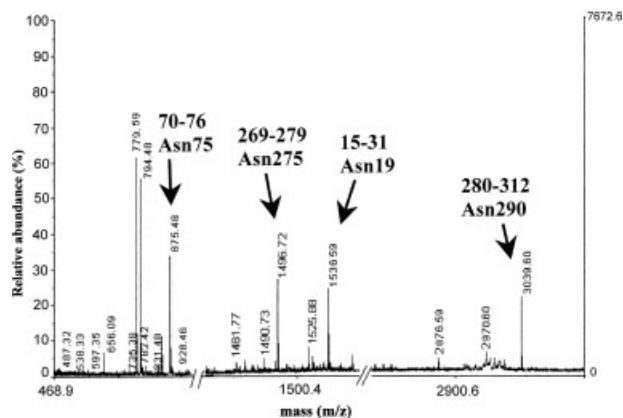
```
                1                        25                        50
kiwi      Ac-TAVTDIVPDVVVAKDGSGNFTTVGAAVAAAKDSSTARFVIYIKEGAYFEY
mung bean -------------------------------------------GAYFEN
carrot    -QSSTVTPNVVVAADGSGDYKTVSEAVAAAPEDSKTRYVIRIKAGVYREN
tomato       IANAVVAQDGTGDYQTLAEAVAAAPDKSKTRYVIYVKRGTYKEN
                                                        *  *  *

                                      75                       100
kiwi      VDVDKKKTNLMFIGDGIGKTWIKGNRSVVDGWTTFRSSTVAVVGTGFIAR
mung bean VEVIRRKTNLMWVGDGIGKTVVKASRNVVDGWTTFQSATVAVVGDGFIAK
carrot    VDVPKKKKNIMFLGDGRTSTIITASKNVQDGSTTFNSATVAAVGAGFLAR
tomato    VEVASNKMNLMIVGDGMYATTITGSLNVVDGSTTFRSATLAAVGQGFILQ
          * *    * * *   ***   *         * ** *** * * * ** **

                                 125              ↓          150
kiwi      GISFENYAGPSKHQAVALRSGADFSAFYQCSFVGYQDTLYVHSLRQFYSE
mung bean GVTFENSAGPSKHQAVALRNGADFSAFYQCSFVAYQDTLYVHSLRQFYRE
carrot    DITFQNTAGAAKHQAVALRVGSDLSAFYRCDILAYQDSLYVHSNRQFFIN
tomato    DICIQNTAGPAKDQAVALRVGADMSVINRCRIDAYQDTLYAHSQRQFYRD
             * **   * * ****** * *   *    *** ** ** ***

                      ↓           175                       200
kiwi      CDVYGTIDFIFGNAAAVLQKCNLYARKPNENQKNIFTAQGRDDPNQNTGI
mung bean CDVYGTVDFIFGNAAAVLQNCNLYARKPNKNQRNLFTAQGREDPNQSTGI
carrot    CFIAGTVDFIFGNAAVVLQDCDIHARRPGSGQKNMVTAQGRTDPNQNTGI
tomato    SYVTGTVDFIFGNAAVVFQKCQLVARKPGKYQQNMVTAQGRTDPNQATGT
            **  ******** * *     ** *    * *  ***** **** **

                                  225↓                       250
kiwi      SILNCKVAAAADLIPVLSSFKTYLGRPWKEYSRTVFLLSQMESLIDPAGW
mung bean SIINCKVAAAADLIPVKSEFRNYLGRPWKMYSRTVFLNSLMEDLIEPAGW
carrot    VIQKSRIGATSDLQPVQSSFPTYLGRPWKEYSRTVVMQSSITNVINPAGW
tomato    SIQFCNIIASSDLEPVLKEFPTYLGRPWKEYSRTVVMESYLGGLINPAGW
            *         *  ** **     *   ****** *****    *   * ****

                                     275                     300
kiwi      LEWSGDFALTTLYYREYKNTGPGSNTTARVTWPGYAVTTNETEVIQFTVG
mung bean LEWNGTFALDTLYYGEYNNRGPGANTSGRVTWPGYRVITNSTEASQFTVQ
carrot    FPWDGNFALDTLYYGEYQNTGAGASGRVTWKGFKVITSSTEAQGFTPG
tomato    AEWDGDFALKTLYYGEFMNNGPGAGTSKRVKWPGYHVITDPAKAMPFTVA
            * *  *** **** *** * *   *  **** *    * *       **

                              321
kiwi      NFIQGSQWLTSYNIPVYLNLT
mung bean NFIQGNEWLNSYGIPFFSGLT
carrot    SFIAGGSWLKATTFPFSLGL-
tomato    KLIQGGSWLRSTGVAYVDGLYD
          * *  **      *
```

Figure 2

Alignment of the sequence of kiwi PME with those of homologous enzymes. Sequences of carrot and tomato PMEs, as well as that of PMEα from mung bean, were obtained from the SWISS-PROT Data Bank, using the accession numbers Q9M5J0, P83218, P14280, respectively. The residues common to all sequences and the residues of the active site are indicated by asterisks and arrows, respectively. N-glycosylation sites are black-shadowed. The residues of tomato PME as well as the corresponding residues of kiwi PME involved in hydrogen bonds and salt-link interactions in the complex formation are gray-shadowed.

led to the complete sequence of the peptide. Mass spectrometry analysis of peptide T1 showed a molecular mass 42 Da higher than that calculated from the amino acid sequence. Therefore, taken together these data indicated that the N-terminal Thr residue of kiwi PME is acetylated.

Peptide T20 (residues 234–268) was eluted in low amount from HPLC, probably due to its low solubility. Direct sequencing of this peptide allowed identification of the first 21 residues. Elucidation of the sequence region going from residue 255 to residue 265 was obtained by sequencing the DP fragment (see Fig. 1) deriving from the acidic cleavage of T20 between Asp246 and Pro247, followed by treatment with OPA (see the Materials and Methods section). The region 263–268 was obtained by direct sequencing of the TP fragment (see Fig. 1) originated from the peptic digestion of T20.

To clearly identify residues that appeared ambiguous, several peptides obtained by chymotryptic proteolysis were separated by reverse phase chromatography and

Figure 3

Partial MALDI/MS spectrum of the tryptic peptide mixture after PNGase A incubation. The peptides containing N-glycosylation sites are indicated.

sequenced. For example, characterization of peptide K1 was useful to confirm the residue Trp82 and the glycosylation consensus sequence at position 75.

Amino acid sequence analysis

It is well known that Asn residues within consensus sequence Asn-X-Ser/Thr, where X is any amino acid except for proline, are potential glycosylation sites.[27,28] Since glycosylated Asn residues provide a blank cycle during automated Edman degradation, we assigned a putative Asn residue when a blank cycle was detected and the residue Asn +2 was Ser or Thr (see Fig. 1).

Kiwi PME sequence comprises 321 amino acids, with a deduced molecular mass of 35.4 kDa. Since the purified protein has an apparent molecular mass of 50 kDa[17] and the primary structure contains N-glycosylation consensus sequences, this discrepancy was ascribed to N-linked oligosaccharides.

Homology search in Data Bank carried out by BLAST showed that kiwi PME sequence shares the highest identity (77%) with mung bean PMEα. Alignment of kiwi PME sequence with the available partial sequence of this protein and with the sequences of tomato and carrot enzymes is shown in Figure 2. The degree of sequence identity with tomato and carrot PMEs is 55 and 56%, respectively.

Identification of N-glycosylation sites

Intact PME was reduced, carboxyamidomethylated under denaturing conditions and digested with trypsin. Glycopeptides were then deglycosylated by incubation with PNGase A and the oligosaccharide mixture was separated from the peptides by a Sep-pack reverse phase chromatographic step. The glycan portion was stored for

further analyses (see below). The peptide mixture was directly analyzed by MALDI/MS, and Figure 3 shows the corresponding partial MALDI mass spectrum. The mass signals were assigned to the corresponding peptides within the PME sequence on the basis of their mass value and the specificity of the enzyme, as reported in Table I.

About 80% of the entire amino acid sequence of PME was confirmed by the mass mapping procedure. Moreover, the glycosylation state of four out of the five putative N-glycosylation consensus sequences occurring in PME structure could also be defined. The mass signal at m/z 875.5, 1496.7, and 3039.6, in fact, occurred 1 Da higher than the expected values for the corresponding 70–76, 266–279, and 286–312 peptides due to the conversion of Asn75, Asn275, and Asn290, respectively, into Asp following PNGase A incubation. On the contrary, the mass signal at m/z 1536.7 perfectly matched the predicted mass value of the peptide 15–31, thus indicating that the Asn residue at position 19 was unmodified. Unfortunately, no information on the glycosylation state of Asn319 could be obtained from these data.

Characterization of PME-linked oligosaccharides

The oligosaccharide mixture released from PME was directly analyzed by MALDI/MS producing the spectrum shown in Figure 4(A). The mass signals recorded in the spectra were tentatively assigned to the putative corresponding oligosaccharide structures, as reported in Table II, on the basis of their known biosynthetic pathway.[29] However, a detailed investigation of the different glycans was performed by tandem MS/MS experiments using MALDI PSD analyses. As an example, Figure 4(B) shows the PSD spectrum of the precursor ion at m/z 2233.2. The spectrum was dominated by Y and B ions containing the nonreducing and the reducing end of the glycan that

Table I

MALDI/MS Analysis of the Tryptic Peptide Mixture After PNGaseA Treatment

| MW$_{expected}$	MW$_{observed}$	Peptide	Note
874.5	875.5	70–76	Asn75 glyc
906.5	906.5	184–191	
1020.6	1020.6	222–229	
1269.6	1269.6	101–112	
1426.8	1426.7	1–14	
1495.7	1496.7	266–279	Asn275 glyc
1536.7	1536.6	15–31	Asn19 unmodified
1555.8	1555.7	222–233	
1562.7	1562.6	44–56	
1616.8	1616.2	178–191	
1690.8	1690.7	44–57	
2045.1	2045.1	101–119	
2121.1	2121.1	58–76	
2576.2	2576.0	184–206	
3018.4	3018.4	120–145	
3038.6	3039.6	286–312	Asn290 glyc
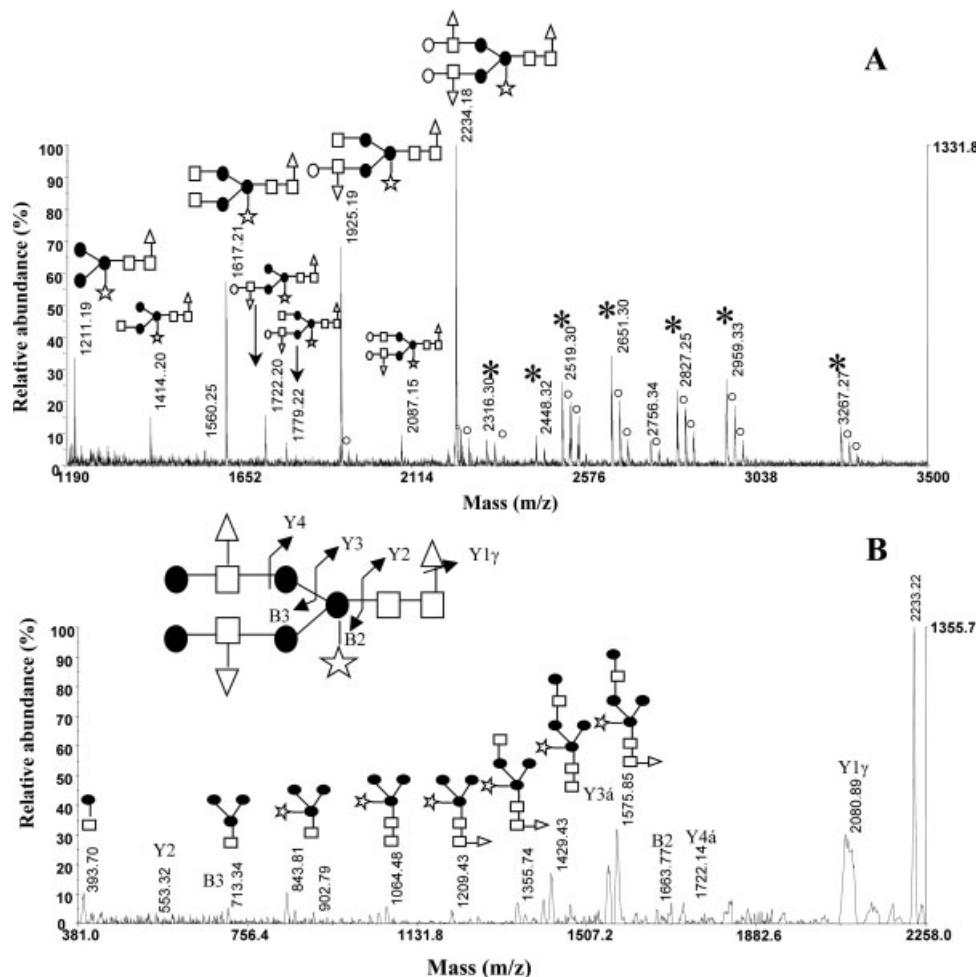
Figure 4

(**A**) MALDI/MS analysis of oligosaccharides released from PME. Species whose structure was not probed by PSD experiments are indicated by an asterisk. Na^{+} adducts are indicated by ○. (**B**) PSD analysis of precursor ion at m/z 2233.22. B and Y fragmentation ion and fragmentation originated by double cleavages are indicated. Triangles, fucose; squares, N-acetylglucosamine; filled/hollow circles, hexose; stars, xylose.

defined the sequence and branching of the antennae. A number of internal fragment ions generated by multiple glycosidic cleavages could also be observed from which the monosaccharide sequence was deduced. These data demonstrated that the glycan structure at m/z 2233.2 was a xylosilated tri-fucosylated biantennary oligosaccharide. The interpretation of the PSD spectra allowed us to confirm the oligosaccharide structures listed in Table II. As shown in the table, the glycans N-linked to PME belong to the complex type oligosaccharides and essentially consist of xylosilated biantennary structures carrying a different number of fucose residues.

Once the glycosylation profile of PME was established, a further step into the structural characterization of this glycosydic moiety consisted in the definition of the site-specificity, that is, the assignment of the glycosylation pattern occurring at each individual Asn residue. Intact

PME was then reduced, carboxyamidomethylated, and digested with trypsin to confine each N-glycosylation site within a single fragment. The resulting glycopeptides were separated by HPLC and each individual fraction was deglycosylated by PNGase A treatment. The oligosaccharides were separated from the peptidic material by HPLC, and both the peptide and the sugar fractions were directly analyzed by MALDI/MS. This procedure led to the definition of the glycosylation state of the last putative N-glycosylation site. The MALDI spectrum of the peptidic material from one of the glycopeptides showed the occurence of a single compound at m/z 1046.5, that was assigned to the fragment 313–321 containing Asn319 converted into Asp following PNGase A hydrolysis. This finding demonstrated that Asn319 is indeed glycosylated.

The MALDI/MS spectra of both the peptidic moiety and the oligosaccharide released from each glycopeptide

Table II

Glycan Structures Detected in the MALDI/MS Analysis of Released Intact PME Oligosaccharides

MW $_{observed}$	Oligosaccharide
MNa$^+$	
1211.19	XylFucHex$_3$HexNAc$_2$
1414.20	FucHex$_3$HexNAc$_3$Xyl
1560.25	Fuc$_2$Hex$_3$HexNAc$_2$Xyl
1617.21	FucHex$_3$HexNAc$_4$Xyl
1722.20	Fuc$_2$Hex$_4$HexNAc$_3$Xyl
1779.22	FucHex$_4$HexNAc$_4$Xyl
1925.19	Fuc$_2$Hex$_4$HexNAc$_4$Xyl
2087.15	Fuc$_2$Hex$_5$HexNAc$_4$Xyl
2234.18	Fuc$_3$Hex$_5$HexNAc$_4$Xyl
MH$^+$	
2316.30	FucHex$_7$HexNAc$_5$
2448.32	XylFucHex$_7$HexNAc$_5$
2519.30	FucHex$_7$HexNAc$_6$
2651.30	XylFucHex$_7$HexNAc$_6$
2756.34	XylFuc$_2$Hex$_8$HexNAc$_5$
2827.25	Fuc$_2$Hex$_8$HexNAc$_6$
2959.33	Fuc$_2$Hex$_8$HexNAc$_6$
3267.27	Fuc3Hex$_9$HexNAc$_6$

led to the assignment of the glycosylation pattern linked to each Asn residue, as reported in Table III.

Influence of pH on the formation of kiwi PME/PMEI complex

The formation of kiwi PME/PMEI complex was studied in the pH range 6.0–10.0 by gel-filtration chromatography. The complex was eluted at a time slightly shorter than that of free PME. Taking advantage of this behavior, the pH conditions prompting the complex formation were investigated. Figure 5 shows the elution profiles

Table III

PME Glycans Sitospecificity

Peptide	MW	Site	Glycoforms
T7 (70–76)	874.5	Asn75	FucHex$_3$HexNAc$_3$Xyl
			FucHex$_3$HexNAc$_4$Xyl
			FucHex$_4$HexNAc$_4$Xyl
			Fuc$_2$Hex$_4$HexNAc$_4$Xyl
			Fuc$_2$Hex$_5$HexNAc$_4$Xyl
			Fuc$_3$Hex$_5$HexNAc$_4$Xyl
T22(269–279)	1074.5	Asn275	Fuc$_2$Hex$_4$HexNAc$_3$Xyl
			Fuc$_2$Hex$_4$HexNAc$_4$Xyl
			Fuc$_3$Hex$_5$HexNAc$_4$Xyl
T23(280–312)	3738.8	Asn290	FucHex$_3$HexNAc$_4$Xyl
			FucHex$_4$HexNAc$_4$Xyl
			Fuc$_2$Hex$_4$HexNAc$_4$Xyl
			FucHex$_5$HexNAc$_4$Xyl
			Fuc$_2$Hex$_5$HexNAc$_4$Xyl
			Fuc$_3$Hex$_5$HexNAc$_4$Xyl
T24(313–321)	1046.5	Asn319	Fuc$_2$Hex$_4$HexNAc$_3$Xyl
			Fuc$_2$Hex$_4$HexNAc$_4$Xyl
			Fuc$_2$Hex$_5$HexNAc$_4$Xyl
			Fuc$_3$Hex$_5$HexNAc$_4$Xyl

obtained at different pH values by using a 6:1 molar excess of PMEI over PME. At pH 6.0, 7.5, and 8.5 PME interacted with PMEI and the complex was eluted as a single component at 19 min. In contrast, at pH 10.0 PME and PMEI were eluted separately at their respective elution times (19.5 and 23.5 min), indicating absence of complex formation. SDS-PAGE analysis confirmed that the peak eluted at 19 min contained both PME and PMEI. Enzyme assay showed that it was devoid of any PME activity, confirming the stability of the enzyme-inhibitor complex.

Models of kiwi PME and of PME/PMEI complex

The 3D structure of kiwi PME was first modeled by using the crystal structure of carrot PME, the only plant
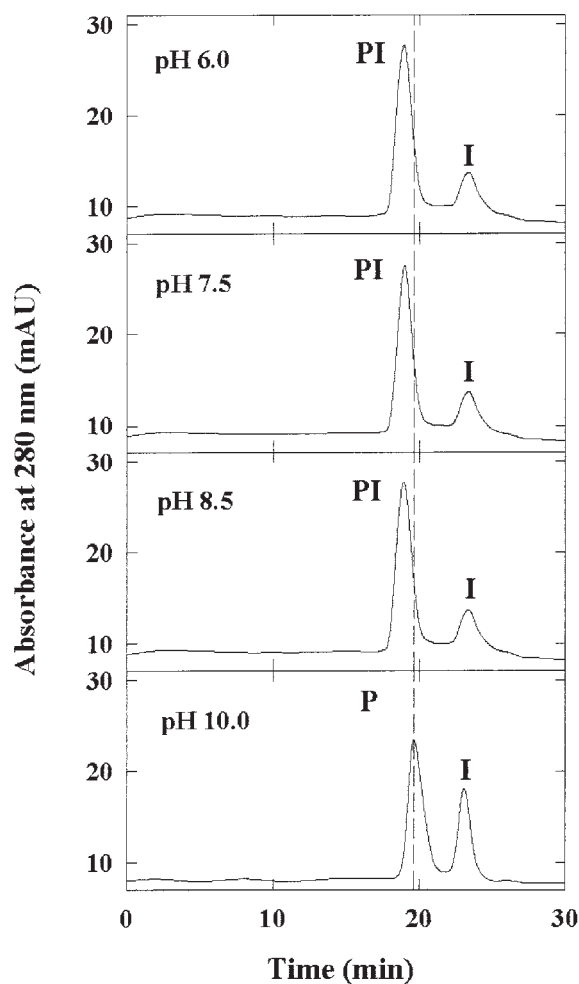
Figure 5

Size-exclusion chromatography of kiwi PME, PMEI, and of the complex PME/PMEI, at the indicated pH values. Free PME, free PMEI, and PME/PMEI complex are indicated by P, I, and PI, respectively. A dashed line indicates the elution time of free PME.

PME structure available at that moment as a template.[12] Following the elucidation of the crystal structure of the tomato PME/kiwi PMEI complex,[10] kiwi PME was also modeled in complex with its inhibitor by using tomato PME as a template. Modeling of the complex showed a minimal displacement of PMEI backbone structure. Superimposition of Cα of all the residues of model and crystal PMEI gave a root-mean-square deviation (rmsd) of 0.10 Å. The Ramachandran plot indicated no residues in PMEI model to be out of the allowed regions.

Analysis of the models and of PME crystal structure indicated a high similarity in the overall folding topology. The analysis of PDF (Probability Density Function) violations performed on the models built in the absence of loop refinement indicated the presence of major violations in loop regions that were largely corrected in the fully refined models. The models that best satisfied the spatial restraints imposed by the program were used for further analysis. Superimposition of Cα of all the aligned residues of the model structure and its crystal template (315 atoms) gave a very low rmsd for both the models built on carrot and on tomato PME (0.38 and 0.19 Å, respectively), thus indicating that kiwi PME sequence well fitted into both structures. The Ramachandran plot indicated only two amino acid residues to be outside the allowed regions in both models.

In both the kiwi PME model structures the residues proposed by Jenkins et al.[11] and Johansson et al.[12] to be part of the catalytic site (Asp137, Asp158, and Arg226 of kiwi PME, corresponding to Asp132, Asp153, and Arg221 of tomato PME) conserved the same position as in tomato and carrot PME structures (see Fig. 2). The four Cys residues of kiwi PME (130,151,171,205) formed an internal polar stacking ladder in the parallel β-helix structure and their position was compatible with the formation of two disulfide bridges between adjacent Cys residues located on parallel beta strands.

Figure 6 shows the distribution of charged and hydrophobic residues on the protein surface of kiwi and tomato PMEs. To highlight the position of the N-linked glycan chains, a PME model was built bearing on Asn75, Asn275, Asn290, and Asn319 a seven-sugar oligosaccharide taken from the *Erythrina corallodendron* lectin structure. The model showed that hydrophobic regions appear to be shielded by the glycan chains (see Fig. 6). It is to underline that the oligosaccharides actually bound to the protein, containing from 9 to 13 sugars, are larger than those we have used in our model, and thus even more effective in the shielding property. No oligosaccharides were observed in the binding site (see Fig. 6). The model of the complex showed that the inhibitor binds kiwi PME in the same site of tomato PME since almost all the H-bonds and the salt links connecting the two proteins in the crystal structure are maintained in our model. The residues found in tomato PME to be involved in H-bonds at the binding site[10] are conserved in kiwi PME with only three exceptions, Lys55 in place of Ser50, Leu144 in place of Gln139, and Asn197 in place of Ala192 (see Fig. 2). Among these substitutions the only one leading to the loss of a H-bond is Leu144, since this residue of kiwi PME is no more able to make H-bond with Ser84 OG of PMEI. Similarly to Ala192 of tomato PME, Asn197 of the kiwi enzyme is involved in a conserved backbone H-bond with the Asn101 side chain of PMEI. In tomato PME, Ser50 is H-bonded to Asp83 (2.97 Å) of PMEI. Kiwi PME has a lysine residue (Lys55) in the same position. This residue, found to lie with its NZ atom between the carboxylic groups of Asp83 and Asp80 of PMEI, binds Asp83 (2.71 Å) forming an interaction stronger than that observed in tomato PME/PMEI complex. Furthermore, Lys55 of kiwi PME forms an additional salt-bridge (3.32 Å) with the carboxylic oxygen of Asp80 (see Fig. 7).

In tomato PME/PMEI complex, the carboxylic group of PME Asp188 is found to be at H-bond distance (2.40 Å) from the carboxylic group of Asp140 of PMEI, thus indicating that they share a proton. In kiwi PME/PMEI complex (see Fig. 7) the corresponding carboxylic oxygen of Asp193 (Asp188 in tomato) is also at H-bond distance (2.84 Å) from Asp140 of PMEI but, differently, it appears to be involved in a salt bridge (3.01 Å) to the guanidinium group of Arg13 of PMEI, located on the N-terminal helical hairpin.[14] Arg13 side chain is slightly displaced with respect to the template structure, due to the presence in kiwi PME of Asp192 (Thr187 in tomato PME) contiguous to Asp193. Arg13 guanidinium group is found to lie between the side chains of the two Asp residues, forming a second salt-bridge (2.98 Å) with Asp192.

DISCUSSION

The apparent molecular mass of purified kiwi fruit PME, determined by gel filtration and SDS-PAGE was reported to be ~50 kDa.[17] Lower values (32–35 kDa) are generally described for homologous plant enzymes.[1] On the basis of the amino acid sequence here reported, the molecular mass calculated for kiwi fruit PME is 35.4 kDa, and therefore falls in the reported range. However, the analysis of the sequence revealed five N-glycosylation consensus sequences suggesting the occurrence of post-translational modifications. Although it is known that PMEs may be glycoproteins, few examples of glycosylated PME are reported. Glycosylation of plant PME has been reported for the acidic enzyme of jelly fig achenes[20] and for the orange thermally tolerant isoenzyme (TT-PME).[18] Jelly fig PME shows an apparent molecular mass of 38 kDa by gel filtration and SDS-PAGE. It has been reported to be presumably N-glycosylated, containing ~10% polysaccharides whose composition has been roughly determined.[20] The recent heterologous expression
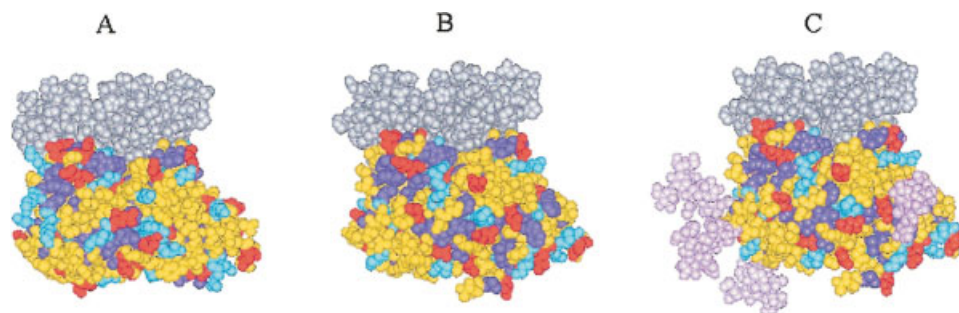
Figure 6

The PME/PMEI complex. Representation of the molecular surface of the complex formed by PME (yellow) and its inhibitor (grey). (**A**) Crystal structure of tomato/kiwi PME/PMEI complex (PDB code 1XG2). (**B**) Model of kiwi/kiwi PME/PMEI complex, built by using 1XG2 as a template. (**C**) Same view of the complex as in (B), with PME bearing on Asn75, Asn275, Asn290, and Asn319 a seven-sugar oligosaccharide (pink). The structures have the same orientation. The models and the crystal template were superimposed by the Cα (315 atoms) of PME and then shifted. The figure shows the distribution of positively charged (blue), negatively charged (red), and hydrophobic (violet) residues on the surface of tomato PME (A) and kiwi PME (B, C). The molecules have been drawn using the Insight II package from Accelrys.

of a functionally active jelly fig PME in a glycosylating system (*Pichia pastoris*) suggested that glycosylation is important for proper folding and stability of the enzyme.[30] The orange TT-PME shows a molecular mass of 40.8 kDa by SDS-PAGE. The neutral PMEα isolated from mung bean (*Vigna radiata*) hypocotyls has an apparent molecular size of 45 kDa[19]; its partial primary structure (deduced from the nucleotide sequence) revealed the presence of four putative N-glycosylation sites, indicating that the enzyme may be glycosylated. Kiwi fruit PME has the highest sequence identity with mung bean PMEα, with which it shares two N-glycosylation consensus sequences.

This article reports the first sequence of plant PME N-glycans. The oligosaccharides linked to the kiwi fruit enzyme have been characterized. Four out of five consensus sequences have been found to be heterogeneously glycosylated. Complex type glycans carrying fucose and xylose moieties have been detected. A higher degree of heterogeneity has been detected in the glycans linked at the level of Asn75 and Asn290, whilst oligosaccharides showing a lower extent of fucosylation and branching constitute the glycan moieties occurring at Asn275 and Asn319. It can be calculated that the glycosylation of kiwi fruit PME approximately accounts for 20% of its molecular mass.

Glycosylation does not seem to affect the catalysis of kiwi fruit PME. In fact, a comparative study carried out with the unglycosylated kaki fruit PME and the kiwi fruit enzyme, showed similar specific activity values and similar salt and pH dependence of activity.[17] Nevertheless,
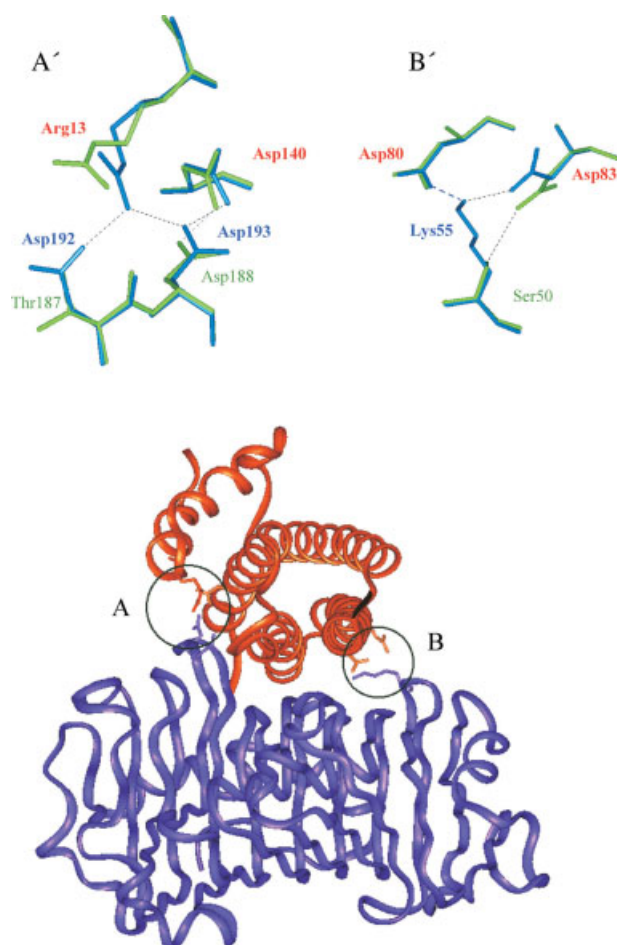

Figure 7

Interaction site of the PME/PMEI complex. In the ribbon representation kiwi PME is in violet and kiwi PMEI is in orange. (**A**, **B**), Regions of the binding site bearing residue substitutions responsible for the specific interaction of kiwi PME with PMEI are circled. (**A′**, **B′**) Close-up view of the circled regions (blue). The corresponding residues of superimposed tomato/kiwi PME/PMEI complex are also shown (green). Residues of kiwi and tomato PME and of PMEI are labeled in blue, green, and red, respectively.

further investigations are necessary in order to verify a possible different behavior with specific substrates.

The catalytic activity of kiwi fruit PME can be completely inhibited following interaction with PMEI, a proteinaceus inhibitor isolated from the same source. PMEI specifically inhibits plant PMEs, forming a 1:1 stoichiometric complex with the enzyme.[16,31] The binding to tomato PME occurs at the active site and the stability of the complex is dependent on pH, being higher at the acidic pH of the apoplasmic environment; the complex formation rapidly decreases in the pH range 6.5–7.5, and is abolished at pH 8.5.[32,33] Conversely, SPR experiments indicated that dissociation of the kiwi PME/PMEI complex at pH values ranging from 3.5 to 8.0 is undetectable, and that complete dissociation occurs only at pH 10.0. The dissociation kinetics observed at pH 9.5 is similar to that observed for tomato PME at pH 7.0.[17] Experiments of size exclusion chromatography, here described, confirmed these results indicating that both free and immobilized kiwi PME are able to form a complex with PMEI, which is stable in a larger pH range than that reported for tomato PME.

To investigate the structural properties of kiwi fruit PME responsible for the high stability of the complex formed with PMEI, modeling of both free and complexed enzyme was carried out. Modeling of kiwi PME/PMEI complex indicated that the inhibitor binding site is the same of tomato PME. In fact, all the H-bonds and the salt-links observed in the crystal structure of tomato PME/PMEI complex to sustain the interaction at the interface between the two molecules are maintained in the modeled kiwi PME/PMEI complex. However, in kiwi PME substitutions of residues located in the loops protruding from the main body of the enzyme, involved in the binding of the inhibitor, may be relevant for the increased stability of the interaction with PMEI. The pH-dependent dissociation of tomato PME/PMEI complex, already observed at neutral pH values, was hypothetically ascribed to the presence of two proton-linked acidic residues, that is, Asp188 of PME, located at the complex interface on TF3 loop[10] (residues 186–193 of tomato PME) and Asp140 of PMEI. In the crystal structure of the complex their carboxylic groups are at H-bond distance, thus indicating that a proton is shared between the two Asp residues. The electrostatic repulsion following deprotonation of the carboxylic groups may loosen the intermolecular H-bond network involving the TF3 loop and destabilize the complex.[10] Modeling of kiwi PME/PMEI complex showed that, similarly to Asp188 of tomato PME, Asp193 of kiwi PME faces Asp140 of the inhibitor. Differently from tomato PME/PMEI complex, a network of ion pairs involving Asp193 and the contiguous Asp192, both located on the TF3 loop of kiwi PME (residues 191–198), and the neighboring Arg13 of PMEI, increases the complex stability. Moreover, the interaction between kiwi PME and PMEI appears to be further stabi-

lized by two additional salt links involving a PME loop on the opposite side of the interaction site with respect to the TF3 loop. These salt links, lacking in tomato PME, occur between Lys55 of kiwi PME, and Asp83 and Asp80 of PMEI. Therefore, it is conceivable that the salt links formed by PMEI Arg13 and PME Lys55, the former located on the inhibitor hairpin, play an important role in the stabilization of kiwi PME/PMEI complex at pH values where tomato PME releases the inhibitor. Thus, the complete dissociation of kiwi PME/PMEI complex observed at high alkaline pH may be correlated to the deprotonation of residues with a pKa close to 10.0, such as lysines and arginines.

Crystallographic data indicate that the N-terminal helical hairpin of PMEI is poorly involved in the interaction with tomato PME, whereas the first approach to the study of the molecular basis of the interaction between kiwi PME and PMEI, here described, suggests that this hairpin (containing the Arg13 residue) is significantly involved in the stabilization of the complex formed by the two partners coming from the same biological source.

N-linked glycans do not interfere with the PME/PMEI binding since they all appear located far from the binding interface. Visual inspection of the protein surface shows that in kiwi PME a number of hydrophobic and uncharged residues, higher than in tomato PME, cluster in the regions bearing glycan moieties. The distribution of the N-linked glycans suggests that they may stabilize the PME structure by shielding areas of the protein surface having a less hydrophilic character. This observation is in line with preliminary results (data not shown) indicating that kiwi PME has higher solubility in aqueous solutions than the tomato homologous enzyme, suggesting a role of polysaccharides in the improvement of protein solubility. In kiwi PME, N-linked glycans could also have a role in the protection of the polypeptide backbone from proteolytic degradation. In fact, the native enzyme is resistant to the proteolysis in conditions where the unglycosylated tomato enzyme undergoes degradation (data not shown).

In conclusion, the investigation of the structural properties of kiwi fruit PME indicates that the molecular mass reported for this enzyme has partly to be ascribed to post-translational modifications of the primary structure. High glycosylation is the most evident structural feature of kiwi fruit PME, lacking in tomato as well as in most plant PMEs known so far. Experimental and modeling data suggest that glycosylation could play a role in the improvement of stability and solubility of kiwi PME. N-glycosylation sites are located far from the catalytic and PMEI-binding site, and the linked oligosaccharides do not appear to affect the enzyme activity and the stronger interaction of kiwi PME with PMEI. Elucidation of the primary structure and modeling of the interaction with the inhibitor indicate that few substitutions in the

amino acid sequence provide additional salt interactions and can be considered the molecular basis of the peculiar high affinity between PMEI and PME from the same biological source.

REFERENCES

1. Micheli F. Pectin methylesterases: cell wall enzymes with important roles in plant physiology. Trends Plant Sci 2001;6:414–419.

2. Giovane A, Quagliuolo L, Castaldo D, Servillo L, Balestrieri C. Pectin methyl esterase from *Actinidia chinensis* fruits. Phytochemistry 1990;29:2821–2823.

3. Gaffe J, Tiznado ME, Handa AK. Characterization and functional expression of a ubiquitously expressed tomato pectin methylesterase. Plant Physiol 1997;14:1547–1556.

4. Micheli F, Sundberg B, Goldberg R, Richard L. Radial distribution pattern of pectin methylesterases across the cambial region of hybrid aspen at activity and dormancy. Plant Physiol 2000;124:191–199.

5. Arabidopsis Genome Initiative. Analysis of the genome sequence of the flowering plant *Arabidopsis thaliana*. Nature 2000;408:796–815.

6. Bosch M, Cheung AY, Hepler PK. Pectin methylesterase, a regulator of pollen tube growth. Plant Physiol 2005;138:1334–1346.

7. Balestrieri C, Castaldo D, Giovane A, Quagliuolo L, Servillo L. A glycoprotein inhibitor of pectin methylesterase in kiwi fruit (*Actinidia chinensis*). Eur J Biochem 1990;193:183–187.

8. Scognamiglio MA, Ciardiello MA, Tamburrini M, Carratore V, Rausch T, Camardella L. The plant invertase inhibitor shares structural properties and disulfide bridges arrangement with the pectin methylesterase inhibitor. J Prot Chem 2003;22:363–369.

9. Giovane A, Servillo L, Balestrieri C, Raiola A, D'Avino R, Tamburrini M, Ciardiello MA, Camardella L. Pectin methylesterase inhibitor. Biochim Biophys Acta 2004;1696:245–252.

10. Di Matteo A, Giovane A, Raiola A, Camardella L, Bonivento D, De Lorenzo G, Cervone F, Bellincampi D, Tsernoglou D. Structural basis for the interaction between pectin methylesterase and a specific inhibitor protein. Plant Cell 2005;17:849–858.

11. Jenkins J, Mayans O, Smith D, Worboys K, Pickersgill RW. Three-dimensional structure of *Erwinia chrysanthemi* pectin methylesterase reveals a novel esterase active site. J Mol Biol 2001;305:951–960.

12. Johansson K, El-Ahmad M, Friemann R, Jörnvall H, Marković O, Eklund H. Crystal structure of plant pectin methylesterase. FEBS Lett 2002;514:243–249.

13. Yoder MD, Keen NT, Jurnak F. New domain motif. The structure of pectate lyase C, a secreted plant virulence factor. Science 1993;260:1503–1507.

14. Hothorn M, D'Angelo I, Marquez JA, Greiner S, Scheffzek K. The invertase inhibitor Nt-CIF from tobacco: a highly thermostable four-helix bundle with an unusual N-terminal extension. J Mol Biol 2004;335:987–995.

15. Hothorn M, Wolf S, Aloy P, Greiner S, Scheffzek K. Structural insights into the target specificity of plant invertase and pectin methylesterase inhibitory proteins. Plant Cell 2004;16:3437–3447.

16. Giovane A, Balestrieri C, Quagliuolo L, Castaldo D, Servillo L. A glycoprotein inhibitor of pectin methylesterase in kiwi fruit. Purification by affinity chromatography and evidence of ripening-related precursor. Eur J Biochem 1995;233:926–929.

17. Ciardiello MA, Tamburrini M, Tuppo L, Carratore V, Giovane A, Mattei B, Camardella L. Pectin methylesterase from kiwi and kaki fruits: purification, characterization and role of pH in the enzyme regulation and interaction with the kiwi proteinaceous inhibitor. J Agric Food Chem 2004;52:7700–7703.

18. Cameron RG, Savary BJ, Hotchkiss AT, Fishman ML. Isolation, characterization, and pectin-modifying properties of a thermally tolerant pectin methylesterase from *Citrus sinensis* var. Valencia J Agric Food Chem 2005;53:2255–2260.

19. Goldberg R, Pierron M, Bordenave M, Breton C, Morvan C, Hervé du Penhoat C. Control of mung bean pectin methylesterase isoform activities. J Biol Chem 2001;276:8841–8847.

20. Ding JLC, Hsu JSF, Wang MMC, Tzen JTC. Purification and glycosylation analysis of an acidic pectin methylesterase in jelly fig (*Ficus awkeotsang*) achenes. J Agric Food Chem 2002;50:2920–2925.

21. Landon M. Cleavage at aspartyl-prolyl bonds. Methods Enzymol 1977;47:145–149.

22. Brauer AW, Oman CL, Margolies MN. Use of *o*-phthalaldehyde to reduce background during automated Edman degradation. Anal Biochem 1984;137:134–142.

23. Greer J. Comparative modeling methods: application to the family of the mammalian serine protease. Proteins 1990;7:317–334.

24. Sali A, Blundell TL. Comparative protein modeling by satisfaction of spatial constraints. J Mol Biol 1993;234:779–815.

25. Naidoo KJ Denysyk D, Brady W. Molecular dynamics simulations of the N-linked oligosaccharide of the lectin from *Erythrina corallodendron*. Protein Eng 1997;10:1249–1261.

26. Friedman M, Krull LH, Cavins JF. The chromatographic determination of cystine and cysteine residues in proteins as s-beta-(4-pyridylethyl)cysteine. J Biol Chem 1970;245:3868–3871.

27. Pless DD, Lennarz WJ. Enzymatic conversion of proteins to glycoproteins. Proc Natl Acad Sci USA 1977;74:134–138.

28. Lerouge P, Cabanes-Macheteau M, Rayon C, Fischette-Laine AC, Gomord V, Fay L. N-glycoprotein biosynthesis in plants: recent developments and future trends. Plant Mol Biol 1998;38:31–48.

29. Jones J, Krag SS, Betenbaugh MJ. Controlling N-linked glycan site occupancy. Biochim Biophys Acta 2005;1726:121–137.

30. Peng CC, Hsiao ES, Ding JL, Tzen JT. Functional expression in *Pichia pastoris* of an acidic pectin methylesterase from jelly fig (*Ficus awkeotsang*). J Agric Food Chem 2005;53:5612–5616.

31. Camardella L, Carratore V, Ciardiello MA, Servillo L, Balestrieri C, Giovane A. Kiwi protein inhibitor of pectin methylesterase. Amino-acid sequence and structural importance of two disulfide bridges. Eur J Biochem 2000;267:4561–4565.

32. Mattei B, Raiola A, Caprari C, Federici L, Bellincampi D, De Lorenzo G, Cervone F, Giovane A, Camardella L. Studies on plant inhibitors of pectin modifying enzymes: polygalacturonase-inhibiting protein (PGIP) and pectin methylesterase inhibitor (PMEI). In: Teeri TT, Svensson B, Gilbert HJ, Feizi T, editors. Carbohydrate bioengineering. Interdisciplinary approaches. Cambridge (UK): The Royal Society of Chemistry; 2002. pp 160–167.

33. D'Avino R, Camardella L, Christensen TMIE, Giovane A, Servillo L. Tomato pectin methylesterase: modeling, fluorescence, and inhibitor interaction studies-comparison with the bacterial (*Erwinia chrysanthemi*) enzyme. Proteins 2003;53:830–839.